Instability Dynamics of Fracture: A Computer Simulation Investigation

Farid F. Abraham, D. Brodbeck, R. A. Rafey, and W. E. Rudge
IBM Research Division, Almaden Research Center, 650 Harry Road, San Jose, California 95120-6099
(Received 28 March 1994)

Implementing molecular dynamics on the IBM SP1 and PVS parallel computers, we have studied the fracture of two-dimensional notched solids under tension using 10^6 atom systems. Many recent laboratory findings occur in our simulation experiments, one of the most intriguing being the dynamic instability of the crack tip as it approaches a fraction of the sound speed. A detailed comparison between laboratory and computer experiments is presented, and microscopic processes are identified. In particular, an explanation for the limiting velocity of the crack being significantly less than the theoretical limit is provided.

PACS numbers: 62.20.Mk

Continuum fracture theory typically assumes that cracks are smooth and predicts that they accelerate to a limiting velocity equal to the Rayleigh speed of the material [1,2]. In contrast, experiment tells us that, in a common fracture sequence, an initially smooth and mirrorlike fracture surface begins to appear misty and then evolves into a rough, hackled region with a limiting velocity of about six-tenths the Rayleigh speed. In some brittle materials, the crack pattern can also exhibit a wiggle of a characteristic wavelength. Recent experiments have clearly shown that violent crack velocity oscillations occur beyond a speed of about one-third the Rayleigh speed and are correlated with the roughness of the crack surface [3–5]. Two different amorphous brittle materials, PMMA (3,4) and soda-lime glass (5) were used. Unlike the PMMA, soda-lime glass has nearly crystalline order at small length scales. Since both materials showed similar fracture behavior, Gross *et al.* concluded that the fracture dynamics may be universal [5], or materials structure independent, and that a dynamical instability of the crack tip governs the crack velocity behavior and the morphology sequence of "mirror, mist, and hackle" [3–5]. All of these features are unexplained using continuum theory, though recent theoretical advances (e.g., by Langer [6] and Marder and Liu [7]) are providing very important insights into this difficult problem. This suggests that a fundamental understanding may require a microscopic picture of the fracturing process. Pioneering atomistic simulations of crack propagation by Ashurst and Hoover [8] and the brittle to ductile transition by Cheung and Yip [9] were too small in size to study the crack stability issue.

With the advent of scalable parallel computers, computational molecular dynamics can be a very powerful tool for providing immediate insights into the nature of fracture dynamics. We have studied two-dimensional triangular solids with up to 1500 atoms on a side, or about one-half of a micron in length. If we were to do three dimensions for an equivalent number of atoms, a cube would be only 130 atoms on a side. But like experiment [3–5], our interest was in studying two-dimensional "mode one" loading. We were able to follow the crack propagation over sufficient time and distance intervals so that a comparison with experiment became feasible. While the laboratory experiments used amorphous materials in order to suppress the possibility that the instability is due to material defects, we used a defect-free 2D crystal: an amorphous packing is not stable for a one-component 2D system.

We refer the reader to Allen and Tildesley [10], Hoover [11], or Abraham [12] for a treatment of the molecular dynamics (MD) simulation technique, including the many procedures for implementing it. MD predicts the motion of a given number of atoms governed by their mutual interatomic interactions described by a continuous potential function and requires the numerical integration of Hamilton's classical equations of motion. We assume that the interatomic forces are described by a Lennard-Jones (LJ) 12:6 potential with a spline cutoff [13]. Quantities are expressed in terms of reduced units: lengths are scaled by the parameter σ, the value of the interatomic separation for which the LJ potential is zero, and energies are scaled by the parameter ϵ, the depth of the minimum of the LJ potential. Reduced temperature is therefore kT/ϵ. Our choice of the simple LJ force law is dictated by our interest in studying the microscopic features of brittle fracture common to a large class of real physical systems. The LJ potential can be used to represent a generic "brittle" material [13]. For the LJ 2D solid [11], the longitudinal sound speed c_l at zero temperature and pressure is ~ 9, and the transverse sound speed $c_t = c_l/\sqrt{3}$. The Rayleigh speed c_R is approximately equal to the transverse sound speed [11]. Our parallel molecular dynamics program is implemented on the IBM PVS using 16 nodes and on the IBM SP1 using 64 nodes. For 2 027 776 atoms, the update time per time step is 0.9 s for the IBM SP1.

Our system is a 2D rectangular slab of atoms with L atoms on a side, where $L = 712$ for the 5×10^5 atom system and 1424 for the 2×10^6 atom system. The slab is initialized at a reduced temperature of 0.0001. A triangular notch of 10 and 20 lattice spacings for the two re-

0031-9007/94/73(2)/272(4)$06.00

spective lengths is cut midway along the lower horizontal slab boundary, and an outward strain rate $\dot{\varepsilon}_x$ is imposed on the outermost columns of atoms defining the opposing vertical faces of the slab. A linear velocity gradient is established across the slab, and an increasing lateral strain occurs in the solid slab. This leads to eventual structural failure of the material, and this failure can take quite different forms, depending on the applied strain rate. The failure could occur by a single fracture (which is seeded by a notch), multiple internal fractures due to the occurrence of voids, as well as "necking" by slippage of atomic rows of atoms. We found that a strain rate of $\dot{\varepsilon}_x = 0.0001$ is sufficiently small for our size systems to prevent multiple fractures accompanying fracture at the notch. With this choice, the solid fails at the notch tip when the solid has been stretched by $\sim 3\%$. Our system has an exaggerated critical strain for tip failure, which is about an order of magnitude larger than experiment [3,4]. This is necessary to achieve a fracture dynamics that is sufficiently fast to follow by molecular dynamics. At the onset of crack motion, the imposed strain rate remains constant (experiment 1) or is set to zero (experiment 2), and the simulation is continued until the growing crack has traversed the total length of the slab.

Our simulation data are much more detailed for the $L = 712$ system where we generated various visualizations to create video movies of the fracture dynamics for experiments 1 and 2. Because of the greater detail, especially in the time evolution, we will describe this size system and mention facts about the larger system. Figures 1 and 2 graphically summarize our nonzero strain rate simulation (experiment 1) for $L = 712$. Figure 1 shows (a) the crack tip position (in units of reduced length) and (b) the crack tip speed (in units of the Rayleigh sound speed), both as a function of reduced time. Figure 1(c) is an expanded view of the crack tip speed for early time. From Fig. 1(a), we find that the crack tip achieves a limiting speed equal to 0.57 of the Rayleigh speed c_R. However, the "instantaneous" tip velocity is very erratic [Fig. 1(b)] after reaching a speed of $0.32c_R$. Before a time of about 70 and a speed less than $0.32c_R$, the acceleration of the crack tip is quite smooth [Fig. 1(c)], but with the onset of the erratic fluctuations of the tip speed, there is significant deceleration of the propagating crack. Each of these features in Figs. 1(a)–1(c) is obtained for experiment 2 and for the larger system ($L = 1424$), and they are in agreement with the experiments of Fineberg *et al.* [3,4]. As in the laboratory experiment, the influence of physical boundaries is a concern when sound and dynamical defects reflect from them. It should be noted that the onset of the instability relative to tip motion ($\delta t = 15$) occurs significantly earlier than it takes sound to travel from the tip to a lateral boundary and return ($\delta t = 80$). Hence, the transition seems to be an intrinsic instability. This is like the laboratory experiments [3,4], and in terms of scaled crack distances adopted by Fineberg *et. al.* [4], the scaled crack extension at this arrival time

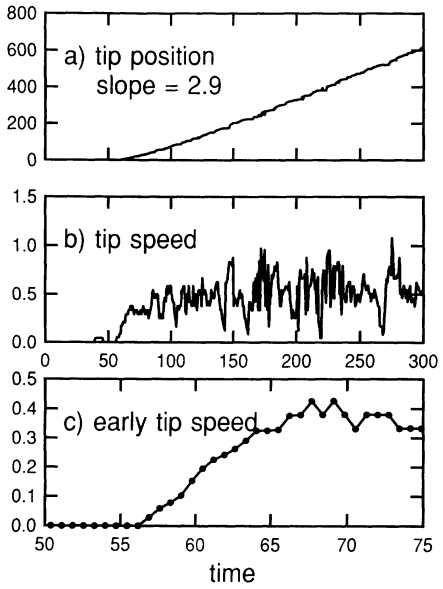

FIG. 1. (a) The crack tip position (in units of reduced length) as a function of reduced time. The slope is the limiting speed in reduced units which corresponds to 0.57 of the Rayleigh speed c_R; (b) the crack tip speed (in units of the Rayleigh sound speed) as a function of reduced time; (c) an expanded view of the crack tip speed for early time.

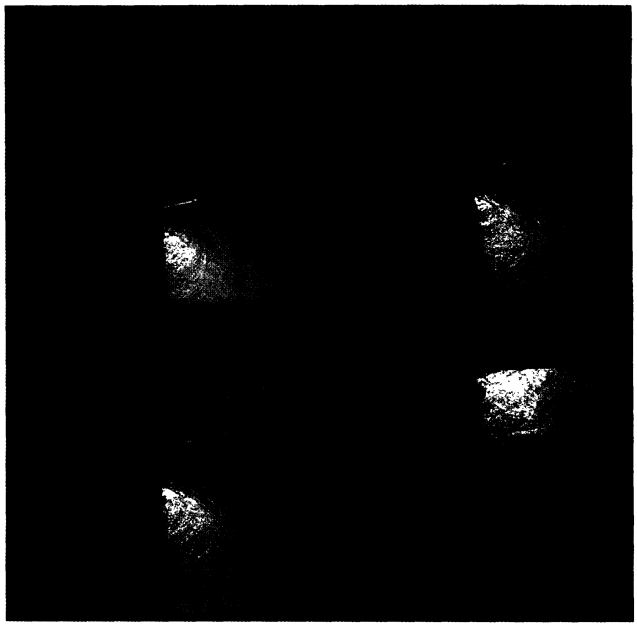

FIG. 2. The time evolution of the propagating crack using a gray-scale rendering of the instantaneous local transverse velocity v_x, or strain rate, which goes from dark gray for the most negative v_x to light gray for the most positive v_x. The time sequence goes from left to right and top to bottom. The frames are for reduced times 140, 180, 200, and 300.

is about the same for our computer simulation and the laboratory experiment.

Figure 2 shows the time evolution of the propagating crack using a gray-scale rendering of the instantaneous local transverse velocity v_x, or transverse strain rate. The scale goes from dark gray for the most negative v_x to light gray for the most positive v_x. Initially, the brittle crack propagates in a straight line and leaves "mirror" cleaved surfaces. Periodic stress waves immediately appear with motion. Corresponding to the onset of the erratic oscillations of the tip speed, at a tip speed of $\sim 0.32c_R$ the crack begins oscillating back and forth at approximate angles of $\leq 30°$ from the vertical (the original direction of crack motion) and along symmetry lines of the crystal. Accompanying the oscillating "zigzag" excursions of the growing crack is significant relaxation in the regions immediately next to the newly created surfaces. Prominent "zigs" or "zags" in the crack direction were accompanied by a propagating atomic displacement along two adjacent rows of atoms that are $\pm 30°$ to the vertical; it is initiated at the vertex of the change of direction and travels at about the longitudinal sound speed c_l. These "dislocations" appear as slanted, inverted V's being emitted from the moving crack tip, first to the right and then to the left. They may be traced back to their origin by constructing an imaginary line 30° from the vertical and passing through the V. The vertical separation between neighboring dislocations equals the wavelength of the oscillating crack and is ~ 115. The V is simply an acoustical wake created by the moving dislocation or dynamic "slip plane." When the dislocation hits the top free boundary, an atomic step is formed. In experiment 1, the solid is being stretched at a nonzero strain rate, and it is "keeping up" with the lateral boundary expansion beyond its elastic limit through the creation and growth of a single crack seeded by the notch, as well as by necking through the slippage of adjacent atomic rows of atoms. For experiment 2 and for $L = 712$, where the imposed strain rate is zero after the onset of crack propagation, we do not observe dislocation emission accompanying the zigzag motion of the crack tip except at the final failure of the slab. However, the failure features of the propagating crack remain qualitatively the same. For experiment 2 and for $L = 1424$, single crack propagation and necking are observed. Increasing the strain during tip propagation (experiment 1) forces the slab to relieve the additional strain by the sliding of atomic rows at each turning point of the crack direction. The dislocations provide an excellent signature for crack oscillation. However, they are not the origin of the oscillation since the same instability behavior is seen in experiment 2.

To highlight the microscopic features of the failure dynamics, we present Fig. 3, which is a short-time interval sequence of close-up views of the crack tip at an early time and at a late time. The crack tip initially propagates straight; then the onset of the crack instability begins as a roughening of the created surfaces which eventually results in the pronounced zigzag tip motion. We refer to these "smooth → rough → zigzag" regions in the crack structure as the microscopic version of "mirror → mist → hackle" seen in experiments at much smaller strains and much larger length scales. In the hackle region, the growth of the fracture is not simply a sharp one-dimensional cleavage progressing in a zigzag manner at 30° from the vertical, or mean crack direction. Instead, we see a stair-step growth of connected "ideal 30° segments," resulting in a net forward angle of about 20° from the horizontal before changing the local direction by $\sim 60°$. The "ideal 30° crack segments" open at a velocity approximately equal to the Rayleigh speed c_R. The origin of the erratic velocity oscillations is associated with the stair-step branching and connecting of regions of failure at and preceding the crack tip. The oscillating zigzag motion of the crack tip and the segmented stair-step growth contribute to the effective "forward" crack speed being less than theoretical prediction. The local fracturing is "brittle" and is the same for experiment 2, with the exception of dislocation emission. While dislocation emission is associated with ductile fracture, it would be misleading to identify experiment 1 as representing ductile fracture and experiment 2 as representing brittle fracture. Unlike ductile fracture, the dislocation creation in experiment 1 is not a governing mechanism for crack opening.

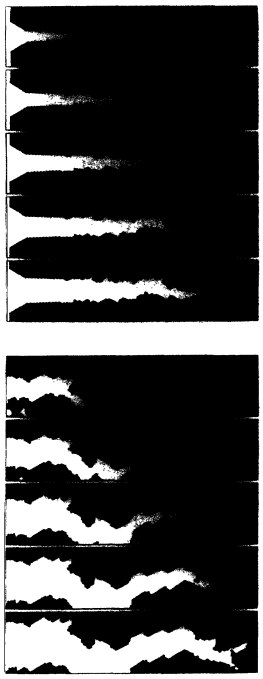

FIG. 3. (a) The onset of crack instability, in reduced time intervals of 7 and beginning at reduced time 85. (b) Late zigzag crack propagation, in reduced time intervals of 7 and beginning at reduced time 220.

This microscopic branching has associated with it

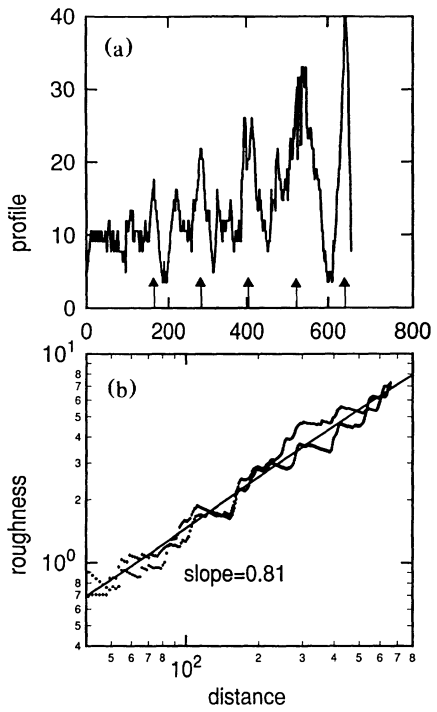

FIG. 4. (a) The profile of a fractured surface and (b) the roughness of the fractured surfaces as a function of crack distance from the originating failure point.

a larger-scale characteristic wavelength and a growing coarse-grain roughness which is shown in Fig. 4. In Fig. 4(a), the profile of a fractured surface is presented as a function of crack distance from the originating failure point, and a wavelength of ~ 115 is apparent. The wavelength of our rough surface is about 2 orders of magnitude smaller than the millimeter wavelength measured by experiment; i.e., λ (simulation) $\sim 10^{-2}\lambda$ (experiment). From the profiles, the roughness, or width, as a function of this distance is calculated [14] and presented in Fig. 4(b). We find that the width w scales with crack distance D, according to the relation $w \sim D^{\zeta}$, where $\zeta = 0.81$. This result is in agreement with recent conjectures of a "universal" roughness exponent for the crack surface of real brittle materials [14].

A detailed comparison between laboratory and computer experiments has been presented. Many of the recent laboratory findings occur in our simulation experiments, one of the most intriguing being the dynamic instability of the crack tip and its associated properties. Microscopic processes have been identified, and explanations of certain features have been suggested, in particular, the reason for the limiting velocity being significantly less than the theoretical limit. Like Gross *et al.*, we conclude that the fracture behavior appears to be universal, or independent of materials structure, simply because we observed many of the laboratory phenomena for our two-dimensional simple atomic system. Of course, as is often the case, the time and length scales in an atomistic simulation are significantly different from typical laboratory experiment. We were forced to accelerate the occurrence of the phenomena, which we did with an order of magnitude increase in strain. In contrast to millimeters and microseconds, we observed the phenomena to occur on scales of tens of nanometers and picoseconds to nanoseconds. However, our "simulation microscope" is validated by comparison and agreement with experiment. As mentioned earlier, the influence of physical boundaries is a concern when sound and dynamical defects reflect from them; e.g., the appearance of Wallner lines on fractured surfaces may occur in brittle materials and are known to be caused by stress waves reflected from nearby surfaces [15]. The dislocations caused the biggest disturbances, and the earliest reflection occurred when the crack was $\sim 70\%$ through the slab. Comparison with the larger system suggests that the immediate effects concerning the overall features of the slab fracture were minor. Going to much larger systems and to three dimensions, developing boundary sinks for disturbances, and employing different interatomic potential functions are very important considerations for future studies in fracture.

Note added.—A multimedia version of this paper is available [16].

[1] *Statistical Models for the Fracture of Disordered Media*, edited by H. J. Herrmann and S. Roux (North-Holland, Amsterdam, 1990).
[2] L. B. Freund, *Dynamical Fracture Mechanics* (Cambridge Univ. Press, New York, 1990).
[3] J. Fineberg, S. P. Gross, M. Marder, and H. L. Swinney, Phys. Rev. Lett. **67**, 457 (1991).
[4] J. Fineberg, S. P. Gross, M. Marder, and H. L. Swinney, Phys. Rev. B **45**, 5146 (1992).
[5] S. P. Gross, J. Fineberg, M. Marder, W. D. McCormick, and H. L. Swinney, Phys. Rev. Lett. **71**, 3162 (1993).
[6] J. S. Langer, Phys. Rev. Lett. **70**, 3592 (1993); J. S. Langer and H. Nakanishi, Phys. Rev. E **48**, 439 (1993).
[7] M. Marder and X. Liu, Phys. Rev. Lett. **71**, 2417 (1993).
[8] W. T. Ashurst and W. G. Hoover, Phys. Rev. B **14**, 1465 (1976).
[9] K. S. Cheung and S. Yip, Phys. Rev. Lett. **65**, 1804 (1990).
[10] M. P. Allen and D. J. Tildesley, *Computer Simulation of Liquids* (Clarendon Press, Oxford, 1987).
[11] Wm. G. Hoover, *Computational Statistical Mechanics* (Elsevier, Amsterdam, 1991).
[12] F. F. Abraham, Adv. Phys. **35**, 1 (1986).
[13] N. J. Wagner, B. L. Holian, and A. F. Voter, Phys. Rev. A **45**, 8457 (1992).
[14] K. J. Måløy, A. Hansen, E. L. Hinrichsen, and S. Roux, Phys. Rev. Lett. **68**, 213 (1992).
[15] A. H. Cottrell, *The Mechanical Properties of Matter* (John Wiley, New York, 1964).
[16] Available via World Wide Web: http://www-i.almaden.ibm.com/vis/fracture/prl.html

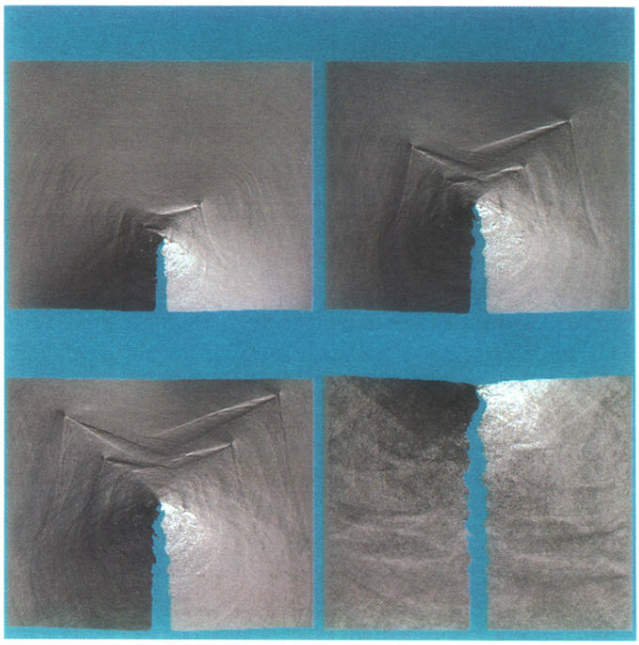

FIG. 2. The time evolution of the propagating crack using a gray-scale rendering of the instantaneous local transverse velocity v_x, or strain rate, which goes from dark gray for the most negative v_x to light gray for the most positive v_x. The time sequence goes from left to right and top to bottom. The frames are for reduced times 140, 180, 200, and 300.